Histochemical observations in Piper malgassicum (Piperaceae) with a special focus on the epidermis

Italian Botanist 12: 29–47 (2021)
doi: 10.3897/italianbotanist.12.70675
https://italianbotanist.pensoft.net

RESEARCH ARTICLE

Italian Botanist
Published by Società Botanica Italiana

Histochemical observations in *Piper malgassicum* (Piperaceae) with a special focus on the epidermis

Emilio Corti[1], Enrico Palchetti[2], Stefano Biricolti[2], Massimo Gori[2,3], Corrado Tani[1], Andrea Squillace[1], Alexander Pittella[1], Alessio Papini[1], Sara Falsini[1]

1 *Dipartimento di Biologia, Università degli studi di Firenze, via P.A. Micheli 3, 50121, Firenze, Italy* **2** *Dipartimento di Scienze e Tecnologie Agrarie, Alimentari Ambientali e Forestali (DAGRI) Università degli Studi di Firenze- Piazzale delle Cascine, 18 – 50144, Firenze (FI), Italy* **3** *Centro Interdipartimentale di Servizi per le Biotecnologie di Interesse Agrario Chimico e Industriale (CIBIACI)-Università degli Studi di Firenze, Via Romana 21 – 50125, Firenze, Italy*

Corresponding authors: Alessio Papini (alessio.papini@unifi.it); Sara Falsini (sara.falsini@unifi.it)

Academic editor: Stefania Biondi | Received 25 June 2021 | Accepted 16 July 2021 | Published 24 September 2021

Citation: Corti E, Palchetti E, Biricolti S, Gori M, Tani C, Squillace A, Pittella A, Papini A, Falsini S (2021) Histochemical observations in *Piper malgassicum* (Piperaceae) with a special focus on the epidermis. Italian Botanist 12: 29–47. https://doi.org/10.3897/italianbotanist.12.70675

Abstract

This is the first contribution about the histochemistry of vegetative and reproductive aerial organs in the genus *Piper* L. *Piper malgassicum* accumulates alkaloids and terpenes in the epidermis and the underlying layers of parenchyma, both in the leaves, in the stems and in anthers. Some idioblasts appear to contain a large amount of secondary metabolites. The micro-anatomical analysis showed peculiar secretory structures both in the leaves, in the anthers and in the ovary. Several lipid aggregates, alkaloid droplets and calcium oxalate crystals were observed in leaves and stems, indicating their role in defence strategies, mechanical support, and pollinators attraction. In the anthers, we observed elaioplasts whose content suggest an alternative and indirect function in pollination and defence against micro-organisms. Besides, some lipid aggregates surrounded by microtubules, detected in the anthers, were recognized as lipotubuloids. The tapetum was of secretory type.

Alkaloids and terpenes were widely distributed in the plant confirming the important biological role of this type of biomolecules and its functional range. In the anthers, terpene and polyphenol inclusions appeared particularly abundant in the epidermal layer, whereas calcium oxalate crystals were observed close to the ovule in the ovary at maturity.

Keywords

anatomy, epidermis, histochemistry, *Piper*, *Piper malgassicum* , plant defence, secondary metabolites, terpenes

Introduction

The genus *Piper* L. belongs to the family Piperaceae and includes more than 2000 species with a pantropical distribution (Quijano-Abril et al. 2006), most of them from America (Ulloa Ulloa et al. 2017). Nowadays, the phylogenetic position of *Piper* as well as of the Piperaceae family, is among the so-called "paleoherbs", a phylogenetically complex basal group of dicots (Loconte and Stevenson 1991; Chase et al. 2016), within the order Piperales (Jaramillo et al. 2008; Palchetti et al. 2018). Piperales are herbaceous or woody plants exhibiting quite primitive morpho-anatomical features (Isnard et al. 2012) *Piper* species can be described either as shrubs, or more frequently, as creepers and lianas in the equatorial regions (Jaramillo et al. 2001). Many *Piper* species present two circles of vascular bundles in the stem, sometimes called polystelic organization, considered as a synapomorphy of the Piperaceae family, except for genus *Verhuellia* (Isnard et al. 2012). The main commercial species are *Piper nigrum* L. native to India, *P. methysticum* (L.) G. Forst. typical of West Polynesia, and *P. cubeba* L. a typical Indonesian species (Maugini et al. 2014). Due to their importance, many species are also cultivated beyond their native geographical region and, in some cases, have become naturalized (Smith et al. 2008). However, species belonging to this genus generally display an exclusive pantropical distribution. They present a high number of growth forms and biomechanical organizations (Isnard et al. 2012) with most species having a restricted area of distribution, while others are widespread (Marquis 2004; Quijano-Abril et al. 2006)

Many species of genus *Piper* have a high economic value all around the world and its trade has a long history, dating back to *ca*. 9,000 years ago. Magnoliids, including Piperaceae, are also characterized by the presence of aromatic compounds like terpenoid essential oils and other odorous volatile substances (Marinho et al. 2011) These substances are found in fruits, seeds, and leaves inside glandular pockets and trichomes, and confer the intense flavour and the characteristic aromatic fragrance in most species of the genus (Ballantini et al. 2018) These chemical components led many species of *Piper* to become an important resource from a commercial point of view. The genus is poorly represented in continental Africa. *P. guineense* Schum. & Thonn. and *P. capense* L. are the only two currently known native and endemic species. In Madagascar, the knowledge of the genus is still incomplete (Palchetti et al. 2018) According to Weil et al. (2017), the non-cultivated species of *Piper* present on the island are *P. heimii* C.DC. and *P. pachyphyllum* Baker, while the presence of *P. borbonense* is not confirmed, even though De Candolle (1923, 1869) assigned some samples from Madagascar (and Mauritius) to this species.

In this contribution, we investigated the vegetative structures and the localization of secondary metabolites of a recently described species of the genus *Piper* L. from Madagascar, *P. malgassicum* Papini, Palchetti, Gori & Rota Nodari (Palchetti et al. 2018, 2020), which is used for the production of local pepper named "voatsiperifery", probably mixed with *P. borbonense* (Miq.) C. DC. and *P. tsarasotrae* Papini, Palchetti, M. Gori & Rota Nodari. For this reason, these species are economically relevant.

Despite extensive knowledge about the secondary metabolites content and a few accounts about the histochemistry of the fruit and seed of *Piper*, particularly *P. nigrum*, there is very limited evidence about the presence of secondary metabolites in the leaves and in general in the epidermis of the organs in the same genus and no data, in general, about *P. malgassicum*. The aim of this study was to correlate anatomical and histochemical features of the epidermis and underlying tissues with secondary metabolite production and defence systems of *P. malgassicum*. We show the anatomical features of the epidermis in leaves, anthers, and ovary using light microscopy (LM) and histochemical techniques. Specific histochemical staining methods were used to localize different classes of secondary metabolites in the vegetative parts of the plants. Since the presence of secondary metabolites in the anthers has been documented rarely, we also used transmission electron microscopy (TEM) to check the local ultrastructural patterns linked to the route of formation of secondary metabolites in the organelles inside anther cell wall cells.

Materials and methods

Plant material

Plants grown from seeds of *P. malgassicum* obtained from Madagascar were grown in a greenhouse at the Department of Agriculture, Food, Environment and Forestry of the University of Florence (Italy) from March to July 2019 at approximately 25 °C during the day of 14 hours and 15 °C during the night of 10 hours under artificial light in a pot (15 cm diameter) containing universal soil plus garden soil (Vigorplant, Italy), without fertilizers; humidity was kept at 70%. The plants were later transferred to the Botanical Garden of Florence (Giardino dei Semplici) Another plant was grown starting from seed directly in the laboratory at room temperature and leaves and stem of the young plant were used for further analysis (vibratome sectioning) After about one month of growth, when stems, leaves, and flowers had reached a suitable size (i.e., 2 mm diameter for the stem, 5 cm length for the leaf, and 1 cm length for the flower) for the light and TEM analyses, sections of leaf, stem, and anthers were cut with a razor blade and a vibratome.

Herbarium samples were made with material directly collected in the field (Vohiday forest, Ambositra region, Madagascar) and conserved at the Tropical Herbarium of Florence, Italy (FT) They are syntypes of the type. For the images, we used sample PS9, Voidahi (Madagascar).

Light microscopy

Leaf and stem sections for LM were cut with a vibratome (Vibratome 1000 Plus) at a thickness of 40–50 μm. Some sections were stained with selective histochemical dyes and reagents for terpenoids and lipophilic substances using Sudan Black for lipid stain-

ing (Lison et al, 1960), NADI for lipids and terpenes (Carde et al. 1964), Sudan Red III-IV for the detection of neutral lipids (Lison et al. 1960), and Fluorol Yellow 088 (FY088) fluorescent staining for lipid detection (Bundrett et al. 1991)

Other sections were stained with selective dyes for non-lipophilic molecules, like polysaccharides, polyphenols, and alkaloids. Schiff's reagent and periodic acid- Schiff (PAS) staining were used for detecting polysaccharides (Jensen 1962), staining with $FeCl_3$ for polyphenols (Strasburger E. 1923) and Wagner's reagent for alkaloids (Wagner and Bladt 1996) Mechanical tissues and other physical support structures were revealed with calcofluor for cellulose staining (Hughes and McCully 1975), phloroglucinol for lignin marking (Johansen 1940), and toluidine blue as generic staining (Beccari and Mazzi 1966) The sections were observed through a Leitz DM-RB "Fluo" light/fluorescence microscope (Wetzler, Germany) equipped with a digital camera (Nikon DS-L1, Tokyo, Japan)

Transmission electron microscopy

Anther samples (about 2 mm long) were collected and fixed in 1.25% glutaraldehyde, at 4 °C, in 0.1 M phosphate buffer (pH 6.8) for 24 h. The samples were fixed in 1% OsO4 in the same buffer for 1 h. After dehydration in an ethanol series and a propylene oxide step, the samples were embedded in Spurr's epoxy resin (Spurr 1969) Cross-sections (about 70-nm thick) were cut with a diamond knife and a Reichert-Jung ULTRACUT ultra-microtome, and then stained with uranyl acetate (Gibbons and Grimstone 1960) and lead citrate (Reynolds 1963) The sections were then examined with a Philips 201 TEM at 80 kV. Semithin sections (1–5 μm), obtained using glass knives, were stained with toluidine blue 0.1%, observed, and photographed.

Results

Macroscopic morphology

The *P. malgassicum* herbarium sample showed simple elongated ovate leaves, while the inflorescences were cylinder-shaped, about 4 cm long. Infructescences were composed of many drupes carried on peduncles inserted orthogonally to the axis (Fig. 1 A, B)

Anatomical observations

Leaf anatomy

P. malgassicum leaves are hypostomatic with dorsoventral mesophyll (Fig. 2A) The upper epidermis is composed of an outer epidermal layer of mostly square cells and an underlying hypodermal layer consisting of rectangular-shaped cells (Fig. 2B) Below, the mesophyll parenchyma was organized in one layer of palisade parenchyma

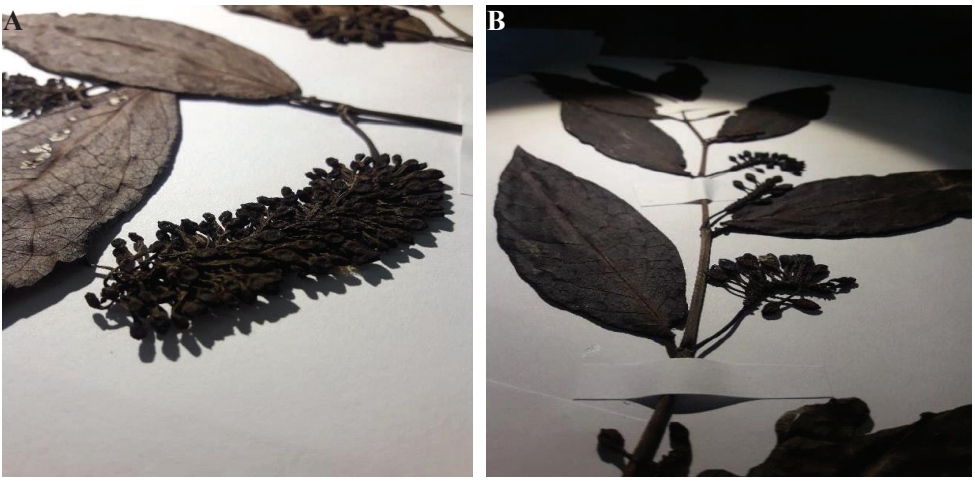

Figure 1. Herbarium specimen of *P. malgassicum* **A** inflorescence **B** leaves and infructescences (sample conserved at the Tropical Herbarium of Florence, University of Florence).

and two or three layers of spongy parenchyma. The tangentially elongated palisade cells were tightly packed and straight or slightly curved. Spongy parenchyma cells were nearly circular, loosely packed, with evident intercellular spaces (Fig. 2C) The abaxial hypodermis was composed of two regions: the epidermis and the hypodermal layer. Cells of the hypodermal layer were either rectangular or irregularly square near the stomata (Fig. 2D) The cells of the abaxial epidermis were either polygonal, circular, or squarish. Stomata (St) and glandular trichomes (Gt) were observed in this region (Fig. 2D)

LM images obtained with polarized light revealed calcium oxalate (CaOx) crystals in the leaf tissue against the dark background (Fig. 2E) CaOx deposits were detected within cells as well as embedded in or associated with the cell wall of midrib vascular bundles in the leaf lamina (Fig. 2F) Some cells of the lower hypodermis accumulated large amounts of CaOx crystals (Fig. 2G) The application of a birefringence filter confirmed that CaOx deposits were found associated with the vascular bundles in the midrib or inside the cells (Fig. 2H) CaOx accumulated in cells of the lower hypodermis immediately below the spongy tissue (Fig. 2I)

Autofluorescence of green leaves in blue light (450–490 nm) resulted in red fluorescence of the chloroplasts due to chlorophyll in all chlorenchyma cells (Fig. 3A, B), including the palisade and spongy mesophyll cells. As expected, red fluorescence was absent in the epidermis and hypodermis. Green fluorescence was attributed to the phenolic components in the cuticle of the upper (adaxial) and lower (abaxial) epidermis as well as in glandular trichomes (Fig. 3A, B) Accordingly, the cell walls of xylem elements in the mesophyll appeared green. Lipid droplets appeared as yellow fluorescence within chlorenchyma cells and in the intercellular spaces, both in the palisade and spongy mesophylls (Fig. 3B). Sudan Black staining also revealed the presence of lipids in the cuticle and inside the trichomes of the lower epidermis (Fig. 3C) Sudan Black

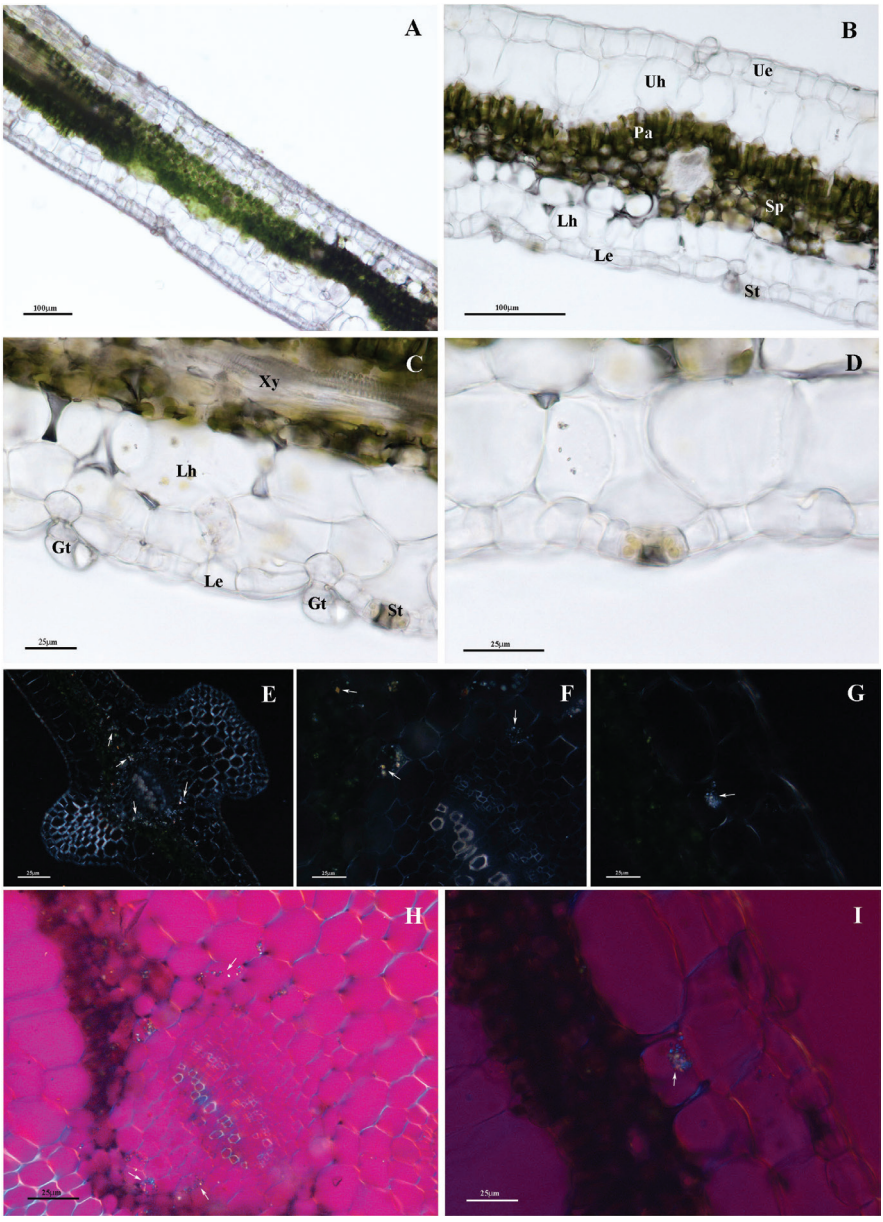

Figure 2. Cross-sections of *P. malgassicum* leaf, LM images **A–D** are cross-section of *P. malgassicum* leaf **F, G** LM observations with polarized light **H, I** LM observations using birefringence filter **A** portion of the leaf lamina **B** detail of image A **C** detail of image B **D** detail of C with stomata **E** portion of the leaf lamina. Presence of CaOx crystals (white arrows) within cells as well as embedded in vascular bundlecell walls **F** cross-section of the leaf through midrib. Abundance of CaOx crystals (white arrows) close to the bundles and embedded in the cell walls of xylemelements **G** presence of CaOx crystals (white arrows) in the lower hypodermis **H** portion of the lamina. CaOx crystals (white arrows) in the lower hypodermis **I** cross-section of the leaf through midrib showing abundant CaOx crystals (white arrow) close to the bundles and embedded in the cell walls of xylemelements. Xy: xylem, Gt: glandular trichomes; Ue: upper/adaxial epidermis, Uh: upper hypodermis, Pa: palisade tissue, Sp: spongy tissue, Lh: lower hypodermis, Le: lower/abaxial epidermis, St: stomata.

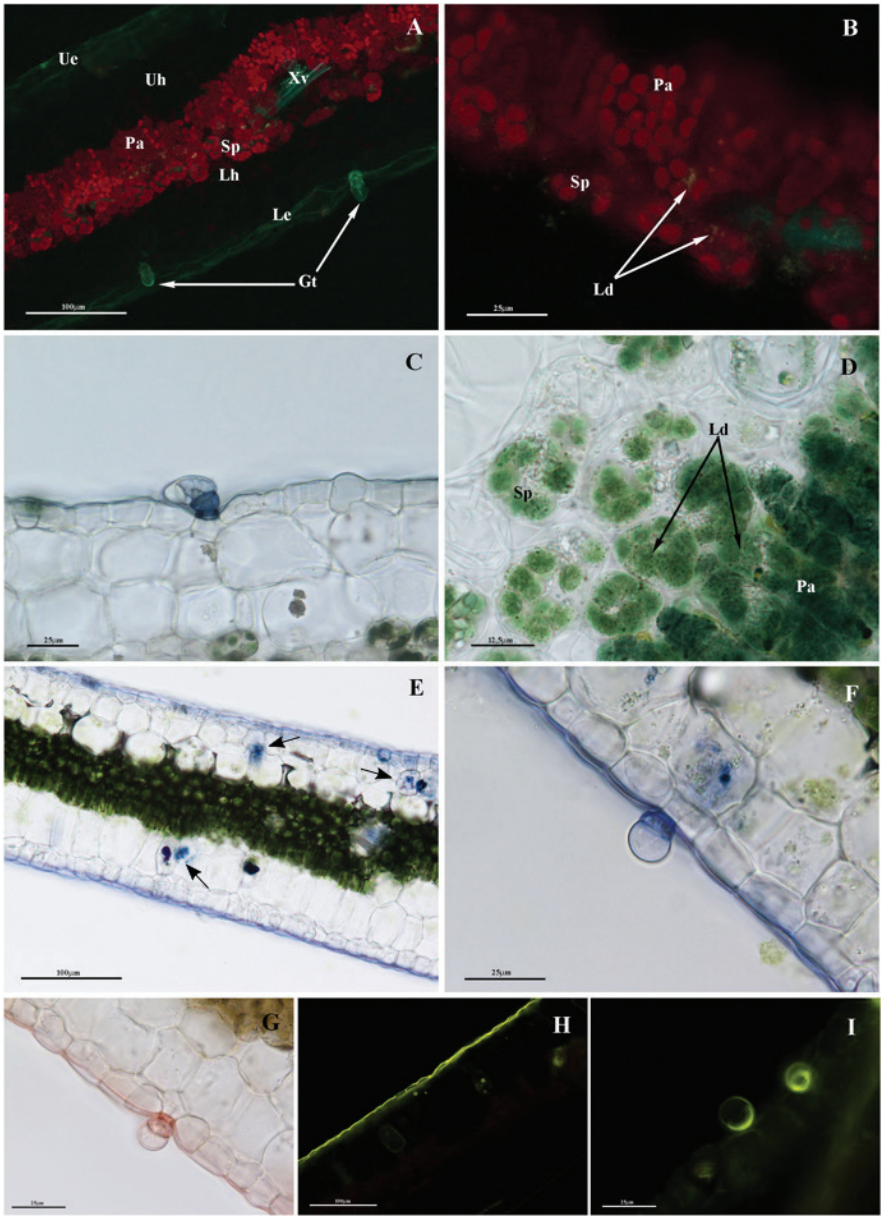

Figure 3. A portion of the leaf lamina in autofluorescence under blue-violet light showing the red fluorescence of chlorophyll and the red fluorescence of the trichome contents **B** detail of image A. Lipid droplets show green fluorescence **C** trichomes and cuticles appearing Sudan Black positive **D** sudan Black stained lipid droplets positively in the spaces between chlorenchyma cells, both in the spongy and the palisade parenchyma (black arrows) **E** leaf stained with NADI reaction. Positive cells can be observed in the mesophyll (arrows) **F** lower epidermis and trichome stained with NADI **G** LM images showing the trichome and cuticle slightly reddish while cutin and suberin resulted stainedbrownish with Sudan III–IV **H** Fluorescence images with Fluorol Yellow staining revealing the lipids in the cuticleand aggregates in the epidermis and mesophyll **I** detail of H): trichome stained with FY088. Ld: lipid droplet; Ue: upper/adaxial epidermis, Uh: upper hypodermis, Pa: palisade tissue, Sp: spongy tissue, Lh: lower hypodermis, Le: lower/abaxial epidermis, Gt: glandular trichomes.

positively stained lipid droplets also in the intercellular spaces of the mesophyll and within cells of both palisade and spongy tissue (Fig. 3D)

As shown in Fig. 3E, NADI staining revealed the presence of a thin NADI-positive layer in correspondence of the leaf cuticle and of aggregates distributed both in the epidermis and in the mesophyll where they were found close to the xylem vessels. NADI-positive trichomes could be observed mainly on the abaxial epidermis (Fig. 3F)

Sudan III-IV staining revealed the presence of neutral lipids in the leaf cuticle and in the glandular trichomes which appeared reddish (Fig. 3G) The suberin and cutin components resulted positively stained with Sudan III–IV, appearing brownish. Fluorol Yellow 088 stained the hydrophobic lipid layer (i.e., cuticle) as well as several lipid aggregates in the epidermis and mesophyll (Fig. 4H) Fluorol Yellow 088-positive material was present also in the glandular trichomes (Fig. 3I).

The PAS reaction revealed the presence of polysaccharide material in the abaxial epidermis at the level of the walls and in the glandular trichomes, which showed an intense pink colour (Fig. 4A, B) Leaf cross-sections stained with FeCl3 did not show any positive reaction, suggesting the absence of polyphenolic compounds (Fig. 4C) The Wagner reaction stained positively the epidermal cells (Fig. 4D, E) and some idioblasts in the upper hypodermis (Fig. 4F), suggesting the presence of alkaloids. A limited number of aggregates were also found in trichome basal cells (Fig. 4G)

Stem anatomy

Piper malgassicum stem showed an epidermis consisting of an outer epidermal layer and an inner hypodermal layer. The outer epidermal cells were tangentially elongated and covered with a thick cuticle (Fig. 5H) Compared to the outer epidermal cells, the hypodermal cells were prismatic and spherical. Beneath the hypodermis, the cortex formed a continuous ring. In the cortex, a 4–5 layered angular collenchyma was present (Fig. 4G) The vascular system showed isolated vascular bundles arranged in two concentric rings. Each ring of cortical bundles was formed, on average, by 7–9 vascular bundles. A smaller ring of 4–5 (on average) medullary bundles was embedded in the parenchyma of the central cylinder. The medullary bundles were larger than the cortical bundles. In general, bundles of both rings showed phloem and xylem vessels separated by fascicular cambium. Phloem cells were at the external periphery of the bundle. The central part of the central cylinder was formed by parenchyma cells with thin walls and an open space or lacuna (no pith cells) was often observed right in the middle (Fig. 4G) LM observation using a birefringence filter showed an abundance of CaOx crystals in the stem hypodermis (Fig. 5A) as well as in the leaf. In particular, CaOx accumulated abundantly in the hypodermis cells (Fig. 5B) Sudan III-IV positively stained the cuticle covering the external epidermis (Fig. 5C) and lipid droplets occurring in the lumen of the phloem within the vascular bundles (Fig. 5D) As shown in Fig. 5E, cellulose components were present in the wall of hypodermis cells. Cell walls reacting positively to calcofluor staining were observed in the cortex and the phloem of both cortical and medullar vascular bundles (Fig. 5F) Due to their lignified cell walls, xylem vessels, stained positive to phloroglucinol, but were negative to calcofluor staining (Fig. 5G, H)

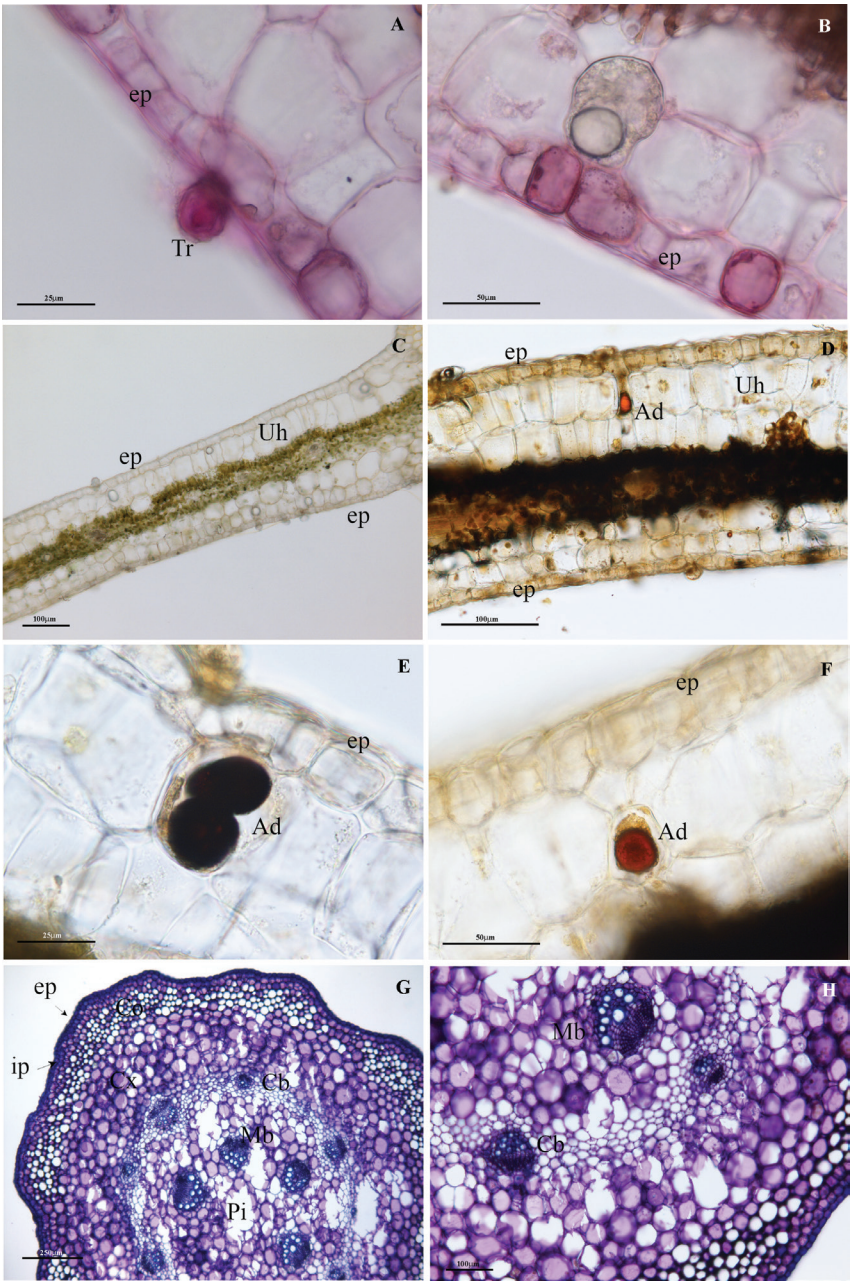

Figure 4. LM images of the cross-sections of *P. malgassicum* leaf (**A–F**) and stem (**G, H**) **A** PAS positivity of trichomes and epidermis cells **B** PAS positivity of the epidermal cells and terpenic droplet below the first layer of cells **C** staining with FeCl3 **D** leaf lamina positive to Wagner staining **E** detail of D showing alkaloid droplets in the hypodermis cell **F** detail of D showing alkaloid droplets in hypodermis idioblasts **G** stem stained with Toluidine blue showing the thick layer of collenchyma beneath the epidermis and the two concentric circles of vascular bundles **H** detail of G showing the wall thickenings of the angular collenchyma. Ad: Alkaloid droplet; Cb: cortical circle of vascular bundles; Co: angular collenchyma; cx: cortex; ep: epidermis; hp: hypodermis; Mb: medullary circle of vascular bundles; Pi: pith; Td: terpenic droplet; Tr: trichome; Uh: upper hypodermis.

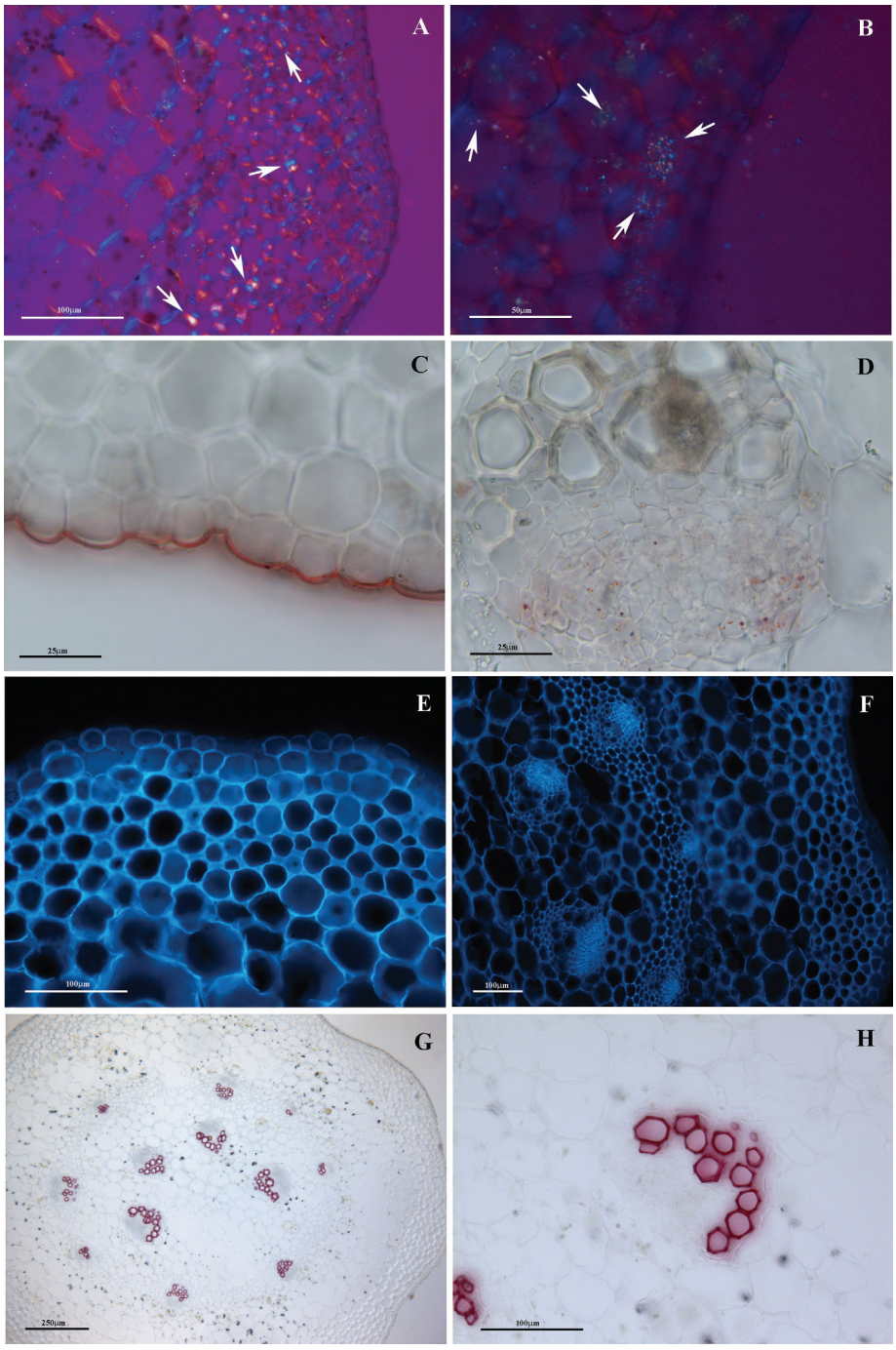

Figure 5. Stem cross-sections **A** CaOx (white arrows) in the hypodermis with birefringence filter **B** detail of A **C** sudan III–IV positive cuticle positive **D** sudan III–IV positive lipid droplets in the primary phloem **E** calcofluor positive (blue fluorescence) hypodermis cell walls **F** cortex and phloem cells walls staining positively withcalcofluor (blue fluorescence) **G** xylem vessels of both cortical and medullary bundles resulted positive to phloroglucinol **H** Detail of G.

Anther anatomy

Piper malgassicum anthers were composed of two locules, joined together by connective tissue. The pollen grains were surrounded by the tapetum and further three cell layers, the epidermis being the most external one (Fig. 6A, B) The anther wall consisted of 2–3 layers of cells, later dehiscing at maturity (Fig. 6A) The tapetum was formed by a monolayered ring of cells, even though, in some points, two cells could be observed (Fig. 6B) Two layers of cells, the middle layer inside and the endothecium outside, just beneath the epidermis, separated the tapetum from the epidermis (Fig. 6B)

The microspores in the locule were surrounded by the tapetum, some of whose cells had a higher electron density than the others (Fig. 6C) Small electron-dense particles (orbicles) were lined along the plasmalemma of tapetal cells, while some larger masses of the same electron density as the orbicles could be observed in the locule and on the microspores (Fig. 6C) Along the anther filaments some trichomes were present. Their cytoplasm contained some plastids with large electron-dense bodies (Fig. 6D) Starch grains (black arrows) were also observed inside these plastids (Fig. 6E) In the epidermis electron-dense bodies were observed in the vacuoles, while some plastids with starch grains were present in the cytoplasm (Fig. 6F) Large medium electron-dense granular bodies could be found between the vacuole and the external plasma membrane (Fig. 6F) The electron-dense masses in the vacuoles occurred as simple bodies (Fig. 6F), or could be surrounded by a more electron transparent crown (Fig. 6G) In some cells, the electron-dense bodies occupied most of the vacuole (Fig. 6H), while some plastids appeared to host bodies of lower electron density as compared with those of the vacuole (Fig. 6H) The electron-dense bodies surrounded by a less electron-dense crown apparently entered the tonoplast coming from large cisternae in the cytoplasm surrounding the vacuole (Fig. 6G) The medium electron-dense bodies appeared to be surrounded by a membrane inside some plastids that were very often observed close to mitochondria (Fig. 7)

The female inflorescence of *P. malgassicum* is a spike; in our sample, it was 3–8 cm long, with a 1–2 cm long peduncle bearing small sessile flowers on a thin axis. The fleshy ovary was surmounted by a two-branched stigma and contained a single ovule (Fig. 8A) Some resin ducts were observed in the ovary while the stigmas showed papillae in the distal portion (Figure 8B) Ovary cells located in proximity of the ovule showed CaOx crystal deposits (Fig. 8C) The spike axis showed two concentric circles of vascular bundles, the external ones were smaller in comparison to the most internal bundles and a lacuna was observed at the centre (Fig. 8D) The phloem elements contained material that stained positive with toluidine blue (Fig. 8E)

Discussion

The observations of *P. malgassicum* herbarium samples showed the typical morphological features of the species and its differences in comparison to the other phylogenetically related species, such as *P. tsarasotrae* and *P guineense*. *P. malgassicum* leaves were

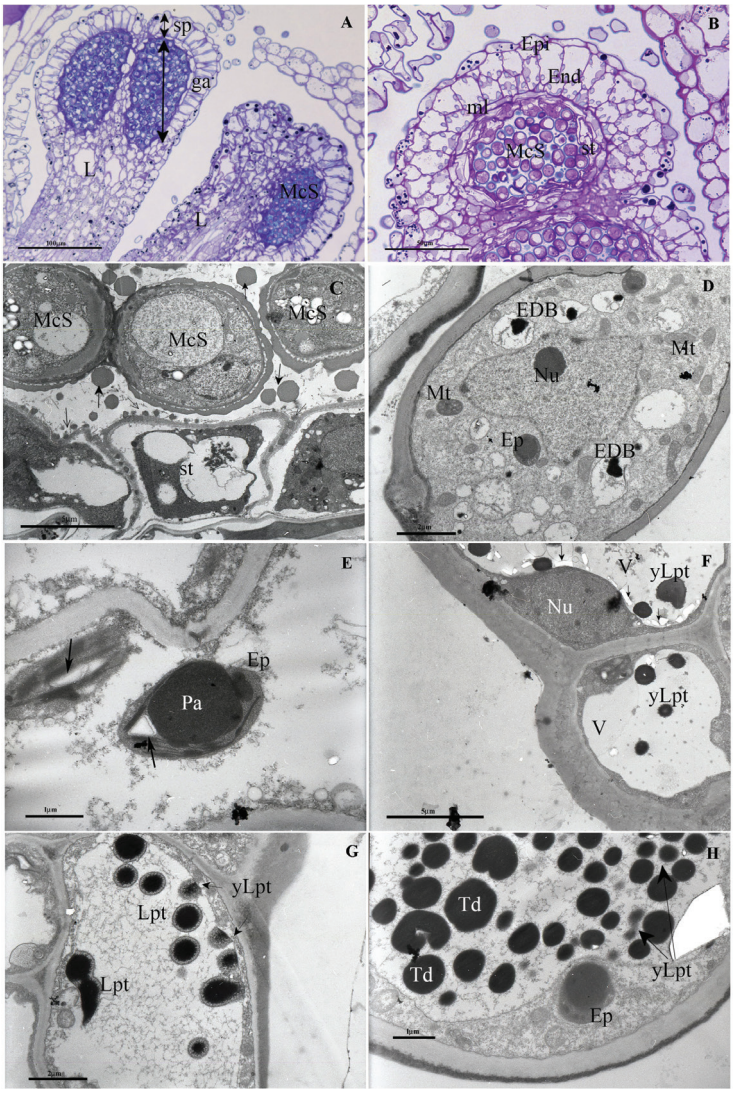

Figure 6. *P. malgassicum* anther **A** Semithin section stained with toluidine blue showing the shape and structure of the anther. Anther wall (here already dehiscent) formed by 2–3 layers of cells **B** semithin section showing the microspores surrounded by the tapetum **C** microspores are in the locule surrounded by the tapetum. Small electron-dense particles (orbicles) are lined along the tapetal cells plasma membrane, while some larger masses can be observed in the locule (black arrow) **D** anther trichome. Some plastids contain large electron-dense bodies **E** detail of D The large electron-dense bodies inside the plastid occur together with starch grains **F** anther epidermis: electron-dense bodies are present in the vacuoles. Some plastids are present with stored starch. Large medium electron dense granular bodies can be found between the vacuole and the external plasma membrane **G** in a preliminary stage, the electron-dense masses in the vacuole are surrounded by a more electron transparent layer **H** at a successive stage, the electron-dense bodies occupy a large part of the vacuolar volume. Ga: microspores/male gametophyte; L: locule; sp: tapetum/sporophytic tissue; ep: epidermis; end: endothecium, ml: middle layer; st: secretory tapetum; Mcs: microspore; EDB: electron-dense bodies; Mt: mitochondria; Pa: protein aggregate; Ep: elaioplast; yLPT: young lipotubule: Lpt: lipotubule; V: vacuole; Td: terpenic droplets.

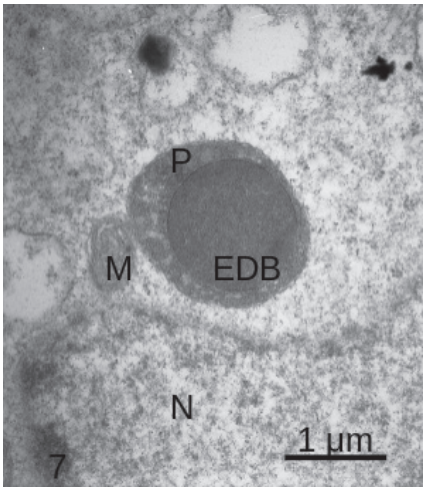

Figure 7. Epidermis cell of anther. A medium electron-dense bodies formed inside a plastid is surrounded by in a membrane and a mitochondrion is very close to the external plastid membrane. EDB: electron-dense Body; M: mitochondrion; N: nucleus; P: plastid.

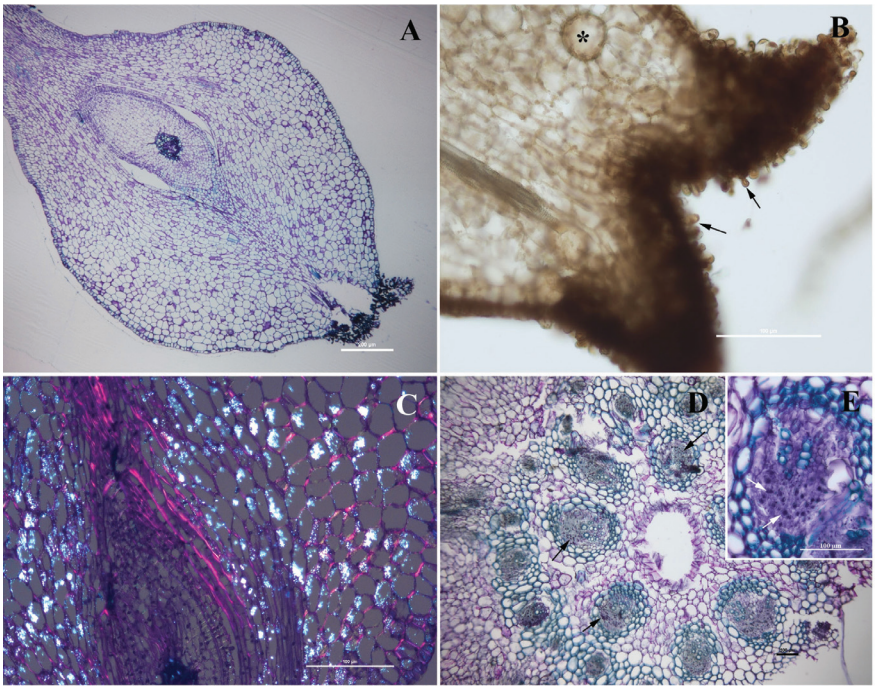

Figure 8. LM image of the longitudinal section of female inflorescence stained with toluidine blue **A** the ovary contains a single ovule and is surmounted by a 2-branched stigma **B** resin ducts as that in the image (asterisk) could be observed in the fleshy ovary. The stigmas were covered with papillae (arrows) **C** CaOx crystals deposits were present in the ovary at maturity **D** female inflorescence spike axis, cross-section. Two concentric circles of vascular bundles, with a lacuna in the middle **E** vascular bundle. Toluidine blue positive material in the phloem.

hypostomatic as in other *Piper* species, such as *P. aduncum* Vell., *P. cernuum* Vell., *P. dilatatum* Rich, *P. gaudichaudianum* Kunth, *P. glabratum* Kunth, *P. lindbergii* C. DC., *P. solmsianum* C. DC., and *P. umbellatum* Jacq. (Gogosz et al. 2012; Raman et al. 2012; Silva et al. 2017; Santos et al. 2018) However, amphihypostomatic leaves were found in *P. sarmentosum* Roxb. (Raman et al. 2012) and amphistomatic in *P. hispidinervum* C. DC (Gogosz et al. 2012) Concerning the anatomical aspects of the leaf, the microscopical analysis revealed how trichomes were not the prevailing secretory structures, but other specialized cells in the hypodermis, called idioblasts, had this function. These cells accumulated lipid-terpenoid aggregates or alkaloids. The general function of these substances and their anatomical localization lead to the hypothesis that their function in *P. malgassicum* is related to the limitation of infections by fungi and bacteria thanks to terpenoids and to the anti-herbivore activity of alkaloids. Most authors studying the genus *Piper* from a phytochemical point of view focussed their attention on the fruit, since it is the most relevant part of the plant for economical purposes. Our observations on the leaves are in agreement with other authors who showed these phytochemical features in other species of the *Piper* genus (Marinho et al. 2011; Pires Jacinto et al. 2018; Silva et al. 2017; Bertocco et al. 2017) From a phytochemical point of view, *P. malgassicum* is closely related to *P. nigrum* (Palchetti et al. 2018, 2020) and used traditionally in the same way as a spice.

Regarding the stem, *P. malgassicum* showed the typical features of Piperaceae family anatomy according to Isnard et al. (2012), but some peculiarities of this species were revealed. The stem showed an angular collenchyma under the epidermal layer organized in smaller areas as compared with other closely-related species of this genus. Probably, the low quantity of collenchyma was due to the young age of the observed *P. malgassicum* stem, which was sectioned after one month of growth from seed. In comparison to *P. malgassicum*, *P. tsarasotrae*, and *P. guineense* showed a higher number of cortical and medullary bundles (Ilodibia et al. 2016; Palchetti et al. 2018) Like *P. tsarasotrae and P. guineense*, *P. malgassicum* has larger medullary bundles than cortical vascular ones. Interestingly, *P. malgassicum*, like *P. guineense* and *P. tsarasotrae*, did not exhibit the mucilage canals observed in other *Piper* species (Ilodibia et al. 2016; Palchetti et al. 2018)

A particular anatomical aspect of *P. malgassicum* was the abundance of CaOx crystals both in the leaves and in the stem. In leaves, these aggregates prevail close to the central rib and in the cells of the spongy mesophyll, while in the stem they were found close to the hypodermis. They were abundant also inside the ovary. Such crystals were also observed in the distantly related *P. callosum* (Silva et al. 2017) and represent a defence against herbivores due to their hardness and spikiness. Moreover, they can provide further mechanical support for the plant (Maugini et al. 2014)

The anthers of *P. malgassicum* displayed the typical characteristics of Magnoliids, in particular, those of the order Piperales (Funes and Randall 2001) In accord with previous studies on others species of *Piper* (Schnarf 1931; Funes and Randall 2001; Valentin-Silva et al. 2015), the anthers of *P. malgassicum* have a secretory tapetum surrounding the microspores. Some of the tapetal cells showed signs of cytoplasmic and

nuclear condensation already at the stage in which microspores are free in the locule. This is evidence of programmed cell death (Brighigna et al. 2006; Papini 2018) and in *P. malgassicum* it appears to occur earlier than in most other angiosperms, where it occurs normally after the first pollen mitotic division (Papini et al. 1999; Varnier et al. 2005; Milocani et al. 2006) LM observations revealed dark globules in the anther epidermis. These organelles with a circular shape could be classified as elaioplasts. The presence of elaioplasts and lipid droplets in anthers is well known (Wu et al. 1999; Suzuki et al. 2013; Quilichini et al. 2014), but mainly within tapetum cells, while in this case they were located in the epidermis. Furthermore, not all the observed dark globules seem to have the typical elaioplast structure. Some of them showed a shape referable to another kind of organelle called lipotubules, according to Kwiatkowska et al. (2012)

The histochemical localization of terpenoids and alkaloids in the leaf epidermis was checked by TEM. Results suggest that the terpenoids accumulated in this tissue involved the activity of plastids, whose electron-dense contents appeared to occupy most of the plastid volume. The tentative identification of the lipid droplets as terpene-containing structures was done on the basis of images from published reports, such as Gersbach (2002, particularly Fig. 7B) and Fahn (1988) The spatial association between plastids and mitochondria may be linked to the functional connection between mitochondrial production of isoprenoids and plastids for the synthesis of terpenoids, namely the 2-C-methyl-D-erythritol-4-phosphate (MEP) pathway observed by Ahn and Pai (2008) in *Nicotiana benthamiana* plastids.

Wagner positivity indicated the presence of alkaloids that can be correlated with the TEM images showing electron-dense bodies found in the vacuole. We could exclude the possible polyphenolic nature of the bodies thanks to the negativity to FeCl3 staining. The images showed that the alkaloids enter into the vacuoles apparently from membrane cisternae probably produced by the endoplasmic reticulum, first with an electron-dense core and a less electron-dense crown. Other images of the vacuole show almost completely electron-dense bodies that are possibly to be referred to a later stage of alkaloids accumulation . Electron-dense precipitates in the vacuoles were interpreted as alkaloids also in *Cataranthus roseus* by Neumann et al (1983), even if in this case the electron-dense bodies were more irregular in shape. Also Ferreira et al. (1998) observed electron-dense bodies in the vavuoles of *Erythroxylum* leaf, interpreting the images (particularly fig. 7 in Ferreira et al. 1998) as accumulation of alkaloids around a more osmiophilic phenolic core. This interpretation may explain the more electron-dense core of the roundish bodies observed in the vacuol of P. malgassicum (our Figure 6G)

The observed NADI positivity could be linked to the production of medium electron-dense material in the plastids. We observed first organelles still containing starch grains (hence confirming their plastidial identity) together with electron-dense masses and, in other cells, possibly at a more advanced stage of development, the enlargement of the electron-dense bodies apparently formed from lipids derived from the thylakoids. Overall, the analysis of *P. malgassicum* has highlighted the presence of peculiar secretory structures in the leaf, thus confirming the aromatic nature of the species and high specialization in the biosynthesis of terpenic substances. However, the abundant

accumulation of lipid globules, alkaloids, and CaOx crystals also points to particular bio-functional strategies of defence, support, and attraction of mutualistic organisms.

In conclusion, our results show that *P. malgassicum* produces secondary metabolites (terpenoids and alkaloids) with defence functions, particularly in the leaf epidermal cells (including trichomes) and in hypodermal idioblasts. This is the first report on the histochemistry of *P. malgassicum* and the first one on the histochemistry of the epidermis in this genus.

References

Ahn C, Pai H-S (2008) Physiological function of a plastid MEP pathway gene for isoprenoid biosynthesis, in organelle biogenesis and cell morphogenesis in *Nicotiana benthamiana*. Plant Molecular Biology 66: 503–517. https://doi.org/10.1007/s11103-007-9286-0

Ballantini S, Innocenti M, Bellumori M, Mulinacci N, Palchetti E (2018) Caratterizzazione fitochimica di nuove specie di pepe selvatico del Madagascar (*Piper malgassicum* e *Piper tsarasotrae*). Tesi di laurea, Università degli Studi di Firenze, 11–18. [/25–40/ 63–66/74–88.]

Beccari N, Mazzi V (1966) Manuale di tecnica microscopica. Soc. Editrice Libraria, Como.

Bertocco ARP, Migacz IP, Santos VLP, Franco CRC, Silva RZ, Yunes RA, Cechinel-Filho V, Budel JM (2017) Microscopic diagnosis of the leaf and stem of *Piper solmsianum* C. DC. Microscopy Research and Technique 80(8): 831–837. https://doi.org/10.1007/s11103-007-9286-0

Brighigna L, Milocani E, Papini A, Vesprini JL (2006) Programmed cell death in the nucellus of *Tillandsia* (Bromeliaceae) Caryologia 59(4): 334–339. https://doi.org/10.1080/00087114.2006.10797935

Bundrett MC, Kendrick B, Peterson CA (1991) Efficient lipid Staining in Plant material with Fluoral Yellow 088 in Polyethylene Glycol-Glycerol, Biotech Histochemistry 66(3): 111–116. https://doi.org/10.3109/10520299109110562

Carde JP, David R (1964) Coloration differentielle des inclusions lipidiques et terpeniques des pseudophylles du Pin maritime on moyen du reactif Nadi. C.R. Acad. Sc. Paris, Ser. D 258: 1338–1340.

Chase MW, Christenhusz MJM, Fay MF, Byng JW, Judd WS, Soltis DE, Mabberley DJ, Sennikov AN, Soltis PS, Stevens PF (2016) An update of the Angiosperm Phylogeny Group classification for the orders and families of flowering plants: APG IV. Botanical Journal of the Linnean Society 181(1): 1–20. https://doi.org/10.1111/boj.12385

De Candolle C (1869) Piperaceae. In: De Candolle C (Ed.) Prodromus Systematis Naturalis Regni Vegetabilis (Vol. 16. Part 1). Masson, Paris, 235–471. [In Latin]

De Candolle C (1923) Piperacearum clavis analytica. Candollea 1: 65–415. [In Latin] https://www.biodiversitylibrary.org/page/15401212

Fahn A (1988) Secretory tissues in vascular plants. New Phytologist 108: 229–257. https://doi.org/10.1111/j.1469-8137.1988.tb04159.x

Ferreira JFS, Duke SO, Vaughn KC (1998) Histochemical and immunocytochemical localization of tropane alkaloids in *Erythroxylum coca* var. *coca* and *E. novogranatense* var. *novogranatense*. International Journal of Plant Sciences 159(3): 492–503. https://doi.org/10.1086/297566

Gersbach PV (2002) The Essential Oil Secretory Structures of *Prostanthera ovalifolia* (Lamiaceae), Annals of Botany 89(3): 255–260. https://doi.org/10.1093/aob/mcf033

Gibbons IR, Grimstone AV (1960) On the flagellar structure in certain flagellate.The Journal of Biophysical and Biochemical Cytology 7: 697–716. https://doi.org/10.1083/jcb.7.4.697

Gogosz AM, Boeger MRT, Negrelle RRB, Bergo C (2012) Comparative leaf anatomy of nine species of the genus *Piper* (Piperaceae). Rodriguésia 63: 405–417. https://doi.org/10.1590/S2175-78602012000200013

Hughes J, McCully ME (1975) The use of an optical brightner in the study of plant structure. Stain Technology 50: 319–329. https://doi.org/10.3109/10520297509117082

Ilodibia CV, Chukwu AJ, Akachukwu EE, Adimonyemma RN, Igboabuchi NA, Ezeabara CA (2016) Anatomical, Proximate, Vitamin and Mineral Studies on *Piper guineense* (Piperaceae), International Journal of Plant & Soil Science 11(1): 1–6. https://doi.org/10.9734/IJPSS/2016/25385

Isnard S, Prosperi J, Wanke S, Wagner ST, Samain MS, Trueba S, Frenzke L, Neinhuis C, Rowe NP (2012) Growth form evolution in Piperales and its relevance for understanding angiosperm diversification: an integrative approach combining plant architecture, anatomy, and biomechanics. International Journal of Plant Sciences 173(6): 610–639. https://doi.org/10.1086/665821

Jacinto ACP, Souza LPD, Nakamura AT, Carvalho FJ, Simao E, Zocoler JL, Bergo CL (2018) Idioblasts formation and essential oil production in irrigated *Piper aduncum*. Pesquisa Agropecuaria Tropical 48(4): 447–452. https://doi.org/10.1590/1983-40632018v4853165

Jaramillo MA, Manos PS (2001) Phylogeny and patterns of floral diversity in the genus *Piper* (Piperaceae) American Journal of Botany 88(4): 706–716. https://doi.org/10.2307/2657072

Jaramillo MA, Callejas R, Davidson C, Smith JF, Stevens AC, Tepe EJ (2008) A Phylogeny of the Tropical Genus *Piper* Using Its and the Chloroplast Intron psbJ–petA. Systematic Botany 33(4): 647–655. https://doi.org/10.1600/036364408786500244

Jensen WA (1962) Botanical Histochemistry. W.H. Freeman & Co Inc., S. Francisco.

Johansen DA (1940) Plant microtechnique. McGraw-Hill Book Co.Inc., N.Y.

Kwiatkowska M, Popłońska K, Wojtczak A, Stępiński D, Polit JT (2012) Lipid body biogenesis and the role of microtubules in lipid synthesis in Ornithogalum umbellatum lipotubuloids. Cell biology international 36(5): 455–462. https://doi.org/10.1042/CBI20100638

Lison L (1960) Histochimie et cytochimie animales (Vol. I). Gauthier-Villars, Paris.

Loconte H, Stevenson DW (1991) Cladistics of the Magnoliidae. Cladistics 7(3): 267–296. https://doi.org/10.1111/j.1096-0031.1991.tb00038.x

Marinho CR, Zacaro AA, Ventrella MC (2011) Secretory cells in *Piper umbellatum* (Piperaceae) leaves: a new example for the development of idioblasts. Flora-Morphology, Distribution, Functional Ecology of Plants 206(12): 1052–1062. https://doi.org/10.1111/j.1096-0031.1991.tb00038.x

Marquis RJ (2004) Biogeography of neotropical *Piper*. Piper: A model genus for studies of phytochemistry, ecology, and evolution. Springer, Boston, 78–96. https://doi.org/10.1007/978-0-387-30599-8_5

Maugini E, Maleci Bini L, Mariotti Lippi M (2014) Botanica Farmaceutica. IX edizione, casa editrice Piccin Padova, Italy.

Milocani E, Papini A, Brighigna L (2006) Ultrastructural studies on bicellular pollen grains of *Tillandsia seleriana* Mez (Bromeliaceae), a neotropical epiphyte. Caryologia 59(1): 88–97. https://doi.org/10.1007/978-0-387-30599-8_5

Neumann D, Krauss G, Hieke M, Gröger D (1983) Indole alkaloid formation and storage in cell suspension cultures of *Catharanthus roseus*. Planta Medica 48(5): 20–23. https://doi.org/10.1055/s-2007-969871

Palchetti E, Gori M, Biricolti S, Masoni A, Bini L, Tani C, Falsini S, Corti E, Papini A (2020) Possible hybrid speciation for two Malagasy species of *Piper* L. (Piperaceae) Caryologia 73(4): 27–38. https://doi.org/10.20944/preprints202009.0083.v1

Palchetti E, Biricolti S, Gori M, Nodari GR, Gandolfi N, Papini A (2018) Two new Malagasy species of genus *Piper* L. (Piperaceae), *Piper malgassicum* and *Piper tsarasotrae*, and their phylogenetic position. Turkish Journal of Botany 42: 4–12. https://doi.org/10.3906/bot-1712-2

Papini A (2018) The investigation of morphological features of autophagy during plant Programmed Cell Death (PCD) In: De gara L, Locato V (Eds) "Plant Programmed Cell Death: Methods and Protocols". Methods in Molecular Biology 1743. Humana Press. https://doi.org/10.1007/978-1-4939-7668-3_2

Papini A, Mosti S, Brighigna L (1999) Programmed-cell-death events during tapetum development of angiosperms. Protoplasma 207: 213–221. https://doi.org/10.1007/BF01283002

Quijano-Abril MA, Callejas-Posada R, Miranda-Esquivel DR (2006) Areas of endemism and distribution patterns for Neotropical *Piper* species (Piperaceae) Journal of Biogeography 33(7): 1266–1278. https://doi.org/10.1111/j.1365-2699.2006.01501.x

Quilichini TD, Douglas CJ, Samuels AL (2014) New views of tapetum ultrastructure and pollen exine development in *Arabidopsis thaliana*. Annals of botany 114(6): 1189–1201. https://doi.org/10.1093/aob/mcu042

Raman V, Galal AM, Khan IA (2012) An investigation of the vegetative anatomy of *Piper sarmentosum*, and a comparison with the anatomy of *Piper betle* (Piperaceae) American Journal of Plant Science 3: 1135–1144. https://doi.org/10.4236/ajps.2012.38137

Reynolds ES (1963) The use of lead citrate at high pH as an electron-opaque stain for electron microscopy. Journal of Cell Biology 17: 208–212. https://doi.org/10.1083/jcb.17.1.208

Santos VLP, Raman V, Bobek VB, Migacz IP, Franco CRC, Khan IA, Budel JM (2018) Anatomy and microscopy of *Piper caldense*, a folk medicinal plant from Brazil. Revista Brasileira de Farmacognosia 28(1): 9–15. https://doi.org/10.1016/j.bjp.2017.11.004

Schnarf K (1931) Vergleichende Embryologie der Angiospermen. Born- traeger, Berlin, 354 pp.

Silva RJF, Aguiar-Dias ACA, Faial KCF, Mendonça MS (2017) Morphoanatomical and physicochemical profile of Piper callosum: valuable assessment for its quality control. Revista Brasileira de Farmacognosia 27: 20–33. https://doi.org/10.1016/j.bjp.2016.07.006

Smith JF, Stevens AC, Tepe EJ, Davidson C (2008) Placing the origin of two species-rich genera in the late cretaceous with later species divergence in the tertiary: a phylogenetic, biogeographic and molecular dating analysis of *Piper* and *Peperomia* (Piperaceae). Plant Systematics and Evolution 275: 20–22. https://doi.org/10.1007/s00606-008-0056-5

Spurr AR (1969) A low-viscosity epoxy resin embedding medium for electron microscopy. Journal of ultrastructure research 26(1–2): 31–43. https://doi.org/10.1016/S0022-5320(69)90033-1

Strasburger E (1923) Das Botanische Prakticum. Fischer, Jena, 883 pp.

Suzuki T, Tsunekawa S, Koizuka C, Yamamoto K, Imamura J, Nakamura K, Ishiguro S (2013) Development and disintegration of tapetum-specific lipid-accumulating organelles, elaioplasts and tapetosomes, in *Arabidopsis thaliana* and *Brassica napus*. Plant science 207: 25–36. https://doi.org/10.1016/j.plantsci.2013.02.008

Ulloa Ulloa C, Acevedo-Rodriguez P, Beck S, Belgrano MJ, Bernal R, Berry PE, Brako L, Celis M, Davidse G, Forzza RC, Gradstein SR, Hokche O, León B, León-Yánez S, Magill RE, Neill DA, Nee M, Raven PH, Stimmel H, Strong MT, Villaseñor JL, Zarucchi JL, Zuloaga FO, Jørgensen PM (2017) An integrated assessment of the vascular plant species of the Americas. Science 358: 1614–1617. https://doi.org/10.1126/science.aao0398

Valentin-Silva A, Coelho VPDM, Ventrella MC, Vieira MF (2015) Timing of pollen release and stigma receptivity period of *Piper vicosanum*: New insights into sexual reproduction of the genus. American Journal of Botany 102(4): 626–633. https://doi.org/10.3732/ajb.1400419

Varnier A-L, Mazeyrat-Gourbeyre F, Sangwan RS, Clément C (2005) Programmed cell death progressively models the development of anther sporophytic tissues from the tapetum and is triggered in pollen grains during maturation. Journal of Structural Biology 152: 118–128. https://doi.org/10.1016/j.jsb.2005.07.011

Wagner H, Bladt S (1996) Plant Drug Analysis: Thin Layer Chromatography Atlas. Springer, Berlin. https://doi.org/10.1007/978-3-642-00574-9

Weil M, Shum Cheong Sing A, Méot JM, Boulanger R, Bohuon P (2017) Impact of blanching, sweating and drying operations on pungency, aroma and color of *Piper borbonense*. Food Chem 219: 274–281. https://doi.org/10.1016/j.foodchem.2016.09.144

Wu SS, Moreau RA, Whitaker BD, Huang AH (1999) Steryl esters in the elaioplasts of the tapetum in developing *Brassica* anthers and their recovery on the pollen surface. Lipids 34(5): 517–523. https://doi.org/10.1007/s11745-999-0393-5